arXiv:cond-mat/0404243v2 [cond-mat.stat-mech] 16 May 2004

Nuclear Spin-Lattice Relaxation in One-Dimensional Heisenberg Ferrimagnets: Three-Magnon versus Raman Processes

Hiromitsu Hori and Shoji Yamamoto
Division of Physics, Hokkaido University, Sapporo 060-0810, Japan

(Received 4 March 2004)

Nuclear spin-lattice relaxation in one-dimensional Heisenberg ferrimagnets is studied by means of a modified spin-wave theory. We consider the second-order process, where a nuclear spin flip induces *virtual spin waves* which are then scattered thermally via the four-magnon exchange interaction, as well as the first-order process, where a nuclear spin directly interacts with spin waves via the hyperfine interaction. We point out *a possibility of the three-magnon relaxation process predominating over the Raman one* and suggest model experiments.

PACS numbers: 75.10.Jm, 75.50.Gg, 76.50.+g

Design of molecule-based ferromagnets is a challenging topic in materials science [1] and numerous quasi-one-dimensional ferrimagnets have been synthesized in this context. Bimetallic chain compounds [2,3] are early examples, one of which has indeed accomplished the three-dimensional ferromagnetic order. Another approach [4] consists of bringing into interaction metal ions and stable organic radicals. Genuine organic ferrimagnets [5,6] were also synthesized. The tetrameric bond-alternating chain compound $\mathrm{Cu(C_5H_4NCl)_2(N_3)_2}$ [7] and the trimeric intertwining double-chain material $\mathrm{Ca_3Cu_3(PO_4)_4}$ [8] are distinct ferrimagnets of topological origin.

Theoretical understanding of one-dimensional ferrimagnets has also significantly been developed [9–14], but very little is known about their dynamic properties yet [15,16]. Although the one-dimensional spin dynamics is a modern topic of great interest [17], systematic calculation of the nuclear magnetic relaxation is still absent. In the late sixties, Pincus and Beeman [18] formulated the nuclear spin-lattice relaxation rate for Heisengerg ferromagnets and antiferromagnets by means of the spin-wave theory and pointed out a significant contribution of the three-magnon scattering to the relaxation rate. However, their theory is not effective in one dimension but is valid at the onset of the three-dimensional long-range order. In such circumstances, modifying the conventional spin-wave theory, we make our first attempt at systematically describing the one-dimensional nuclear spin dynamics on the basis of the spin-wave picture. We predict that *the three-magnon relaxation process should predominate over the Raman one at high temperatures and weak fields in one-dimensional Heisenberg ferrimagnets.*

First of all our scheme [12,19] of modifying the spin-wave theory is distinct from the original idea proposed by Takahashi [20] and Hirsch *et al.* [21]. In the original way of suppressing the divergence of the sublattice magnetizations, a Lagrange multiplier is first introduced and then the effective Hamiltonian is diagonalized subject to zero staggered magnetization. The thus-obtained energy spectrum depends on temperature and fails to describe the Schottky peak of the specific heat [22]. In order to obtain better thermodynamics, we first diagonalize the Hamiltonian, keeping the dispersion relations free from temperature, and then introduce a Lagrange multiplier so as to minimize the free energy. This scheme works well for ferrimagnets, as demonstrated in Fig. 1. Both the approaches well reproduce the magnetic susceptibilty, but our new shceme is much better than the original one at describing the specific heat. The nonvanishing specific heat at high temperatures, that is, the endlessly increasing energy with temperature, is a fatal weak point of the original scheme.

We consider Heisenberg ferrimagnetic chains of alternating spins S and s, as described by the Hamiltonian

$$\mathcal{H}=\sum_{n=1}^{N}\Big[J\boldsymbol{S}_n\cdot\big(\boldsymbol{s}_{n-1}+\boldsymbol{s}_n\big)-g\mu_{\mathrm{B}}H\big(S_n^z+s_n^z\big)\Big]\,. \quad (1)$$

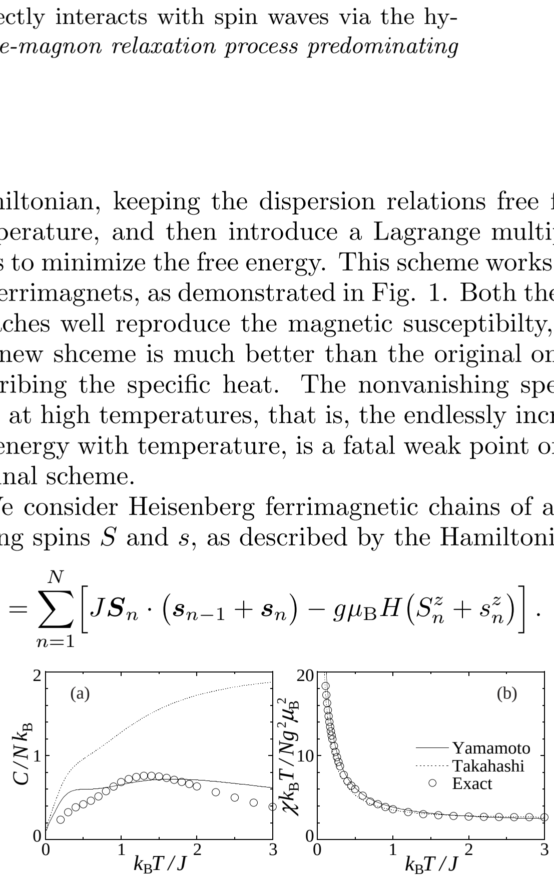

FIG. 1. Modified spin-wave calculations of the specific heat and the magnetic susceptibility as functions of temperature for the spin-$(\frac{5}{2},\frac{1}{2})$ ferrimagnetic Heisenberg chain. The original (Takahashi) and our new (Yamamoto) schemes are compared with numerical findings (Exact) [10].

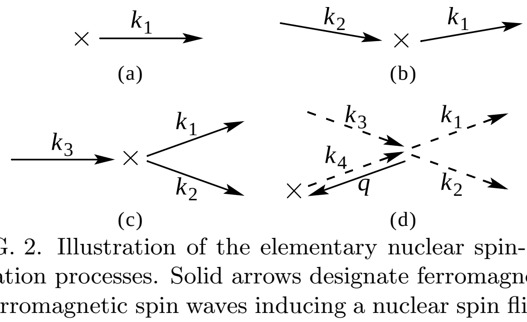

FIG. 2. Illustration of the elementary nuclear spin-lattice relaxation processes. Solid arrows designate ferromagnetic or antiferromagnetic spin waves inducing a nuclear spin flip (×). Broken arrows denote the four-magnon exchange interaction. (a) The direct process. (b) The first-order Raman process. (c) The first-order three-magnon process. (d) The second-order three-magnon process, where $q=-k_4\equiv k_3-k_2-k_1$.

Introducing the Fourier-transformed Holstein-Primakoff magnon operators a_k and b_k for each sublattice, we expand the Hamiltonian with respect to $1/S$ as $\mathcal{H} = \mathcal{H}_2 + \mathcal{H}_1 + \mathcal{H}_0 + O(S^i)$, where we assume that $O(S) = O(s)$ and $\mathcal{H}_i$ contains the $O(S^i)$ terms. The $O(S^{-1})$ contributions are neglected in the following. The hyperfine interaction is assumed to be of the dipolar type as

$$\mathcal{H}_{\mathrm{hf}} = g\mu_{\mathrm{B}}\hbar\gamma_{\mathrm{N}} I^{+} \times \sum_{n=1}^{N} \Big[\frac{1}{2}\big(A_n^{-} S_n^{-} + B_n^{-} s_n^{-}\big) + A_n^z S_n^z + B_n^z s_n^z \Big], \quad (2)$$

where A_n^{σ} and B_n^{σ} are the hyperfine coupling tensors between the nuclear and electronic spins.

Since $\mathcal{H}_0$ and $\mathcal{H}_{\mathrm{hf}}$ are both much smaller than $\mathcal{H}_1$, we may regard $\mathcal{H}_0 + \mathcal{H}_{\mathrm{hf}} \equiv \mathcal{V}$ as perturbative interactions to the linear spin-wave system

$$\mathcal{H}_2 + \mathcal{H}_1 = -2SsJN - (S+s)JN - g\mu_{\mathrm{B}}H(S-s)N + J\sum_k \omega_k + J\sum_k \big(\omega_k^{-} \alpha_k^{\dagger}\alpha_k + \omega_k^{+}\beta_k^{\dagger}\beta_k\big), \quad (3)$$

where $\alpha_k^{\dagger} \equiv a_k^{\dagger}\mathrm{cosh}\theta_k + b_k \mathrm{sinh}\theta_k$ and $\beta_k^{\dagger} \equiv a_k \mathrm{sinh}\theta_k + b_k^{\dagger}\mathrm{cosh}\theta_k$, provided $\tanh 2\theta_k = 2\sqrt{Ss}\cos(k/2)/(S+s)$, create the ferromagnetic and antiferromagnetic spin waves of momentum k, respectively, whose energies are given by $\omega_k^{\sigma} = \omega_k + \sigma(S-s) - \sigma g\mu_{\mathrm{B}}H$ with $\omega_k \equiv [(S-s)^2 + 4Ss\sin^2(k/2)]^{1/2}$. We calculate the thermal distribution functions, $\langle \alpha_k^{\dagger}\alpha_k\rangle \equiv \bar{n}_k^{-}$ and $\langle \beta_k^{\dagger}\beta_k\rangle \equiv \bar{n}_k^{+}$, by enforcing the zero staggered-magnetization constraint [12]. If we consider up to the second-order perturbation with respect to $\mathcal{V}$, the probability of a nuclear spin being scattered from the state of $I^z = m$ to that of $I^z = m+1$ is expressed as

$$W = \frac{2\pi}{\hbar}\sum_f \left| \Big\langle f \Big| \mathcal{V} + \sum_{m(\neq i)} \frac{\mathcal{V}|m\rangle\langle m|\mathcal{V}}{E_i - E_m} \Big| i \Big\rangle \right|^2 \delta(E_i - E_f), \quad (4)$$

where i and f designate the initial and final states of the electronic-nuclear spin system described by the unperturbed Hamiltonian. The nuclear spin-lattice relaxation time is then given by $T_1 = (I-m)(I+m+1)/2W$. Equation (4) contains various elementary relaxation processes, which are illustrated in Fig. 2. Due to the electronic-nuclear energy conservation, the direct process, involving a single spin wave, is rarely of significance. Within the first-order mechanism, where a nuclear spin directly interacts with spin waves via the hyperfine interaction, the three-magnon relaxation rate is much smaller than the Raman one [18]. However, the first-order relaxation rates are generally enhanced through the second-order mechanism, where a nuclear spin flip induces *virtual spin waves* which are then scattered thermally via the four-magnon exchange interaction. We consider the leading second-order relaxation, that is, the exchange-scattering-induced three-magnon process, as well as the first-order relaxation. The second-order relaxation of the Raman type originates in two virtual spin waves within the present model and is therefore negligible in our argument.

Because of the significant difference between the electronic and nuclear energy scales, $\hbar\omega_{\mathrm{N}} \ll J\omega_k^{-} < J\omega_k^{+}$, the intraband spin-wave scatterings determine the Raman relaxation rate $1/T_1^{(2)}$, whereas both the intraband and interband spin-wave scatterings are relevant to the three-magnon relaxation rate $1/T_1^{(3)}$. Assuming the Fourier components of the coupling constants to have little momentum dependence as $\sum_n \mathrm{e}^{\mathrm{i}kn} A_n^{\sigma} \equiv A_k^{\sigma} \simeq A^{\sigma}$ and $\sum_n \mathrm{e}^{\mathrm{i}kn} B_n^{\sigma} \equiv B_k^{\sigma} \simeq B^{\sigma}$, we obtain

$$\frac{1}{T_1^{(2)}} \simeq \frac{2(g\mu_{\mathrm{B}}\hbar\gamma_{\mathrm{N}}B^z)^2}{\hbar JN} \sum_{k_1}\sum_{\sigma=\pm}\sum_{\tau=\pm} X^{\sigma}(\tau k_2^{\sigma}, k_1)^2 \times \bar{n}_{k_1}^{\sigma}(\bar{n}_{k_2^{\sigma}}^{\sigma} + 1) \left| \frac{\mathrm{d}\omega_k^{\sigma}}{\mathrm{d}k} \right|_{k=k_2^{\sigma}}^{-1}, \quad (5)$$

$$\frac{1}{T_1^{(3)}} \simeq \frac{(g\mu_{\mathrm{B}}\hbar\gamma_{\mathrm{N}}B^{-})^2}{16\hbar SJN^2} \sum_{k_1,k_2}\sum_{\sigma=\pm}\sum_{\tau=\pm} 2^{\sigma(\sigma-1)/2} \times Y^{\sigma}(\tau k_3^{\sigma}, k_2, k_1)^2 \bar{n}_{k_1}^{\sigma}\bar{n}_{k_2}^{-}(\bar{n}_{k_3^{\sigma}}^{\sigma} + 1) \left| \frac{\mathrm{d}\omega_k^{\sigma}}{\mathrm{d}k} \right|_{k=k_3^{\sigma}}^{-1}, \quad (6)$$

where k_2^{σ} and k_3^{σ} are given by $\omega_{k_1}^{\sigma} - \omega_{k_2^{\sigma}}^{\sigma} - \hbar\omega_{\mathrm{N}}/J = 0$ and $\omega_{k_1}^{\sigma} + \omega_{k_2}^{-} - \omega_{k_3^{\sigma}}^{\sigma} - \hbar\omega_{\mathrm{N}}/J = 0$, respectively, and

$$X^{-}(k_1,k_2) = \frac{A^z}{B^z}\mathrm{ch}\theta_{k_1}\mathrm{ch}\theta_{k_2} - \mathrm{sh}\theta_{k_1}\mathrm{sh}\theta_{k_2}, \quad X^{+}(k_1,k_2) = \frac{A^z}{B^z}\mathrm{sh}\theta_{k_1}\mathrm{sh}\theta_{k_2} - \mathrm{ch}\theta_{k_1}\mathrm{ch}\theta_{k_2}, \quad (7)$$

$$Y^{-}(k_1,k_2,k_3) = \frac{A^{-}}{B^{-}}\mathrm{ch}\theta_{k_1}\mathrm{ch}\theta_{k_2}\mathrm{ch}\theta_{k_3} - \sqrt{\frac{S}{s}}\mathrm{sh}\theta_{k_1}\mathrm{sh}\theta_{k_2}\mathrm{sh}\theta_{k_3} - \frac{2SV_1(k_1,k_2,k_3,k_3+k_2-k_1)}{J\omega_{k_3+k_2-k_1}^{-} - \hbar\omega_{\mathrm{N}}} \times \Big(\frac{A^{-}}{B^{-}}\mathrm{ch}\theta_{k_3+k_2-k_1} - \sqrt{\frac{s}{S}}\mathrm{sh}\theta_{k_3+k_2-k_1}\Big) - \frac{SV_2(k_1,k_2,k_3,k_3+k_2-k_1)}{J\omega_{k_3+k_2-k_1}^{+} + \hbar\omega_{\mathrm{N}}}\Big(\frac{A^{-}}{B^{-}}\mathrm{sh}\theta_{k_3+k_2-k_1} - \sqrt{\frac{s}{S}}\mathrm{ch}\theta_{k_3+k_2-k_1}\Big),$$

$$Y^{+}(k_1,k_2,k_3) = 2\Big(\frac{A^{-}}{B^{-}}\mathrm{sh}\theta_{k_1}\mathrm{ch}\theta_{k_2}\mathrm{sh}\theta_{k_3} - \sqrt{\frac{S}{s}}\mathrm{ch}\theta_{k_1}\mathrm{sh}\theta_{k_2}\mathrm{ch}\theta_{k_3}\Big) - \frac{SV_3(k_3+k_2-k_1,k_3,k_2,k_1)}{J\omega_{k_3+k_2-k_1}^{-} - \hbar\omega_{\mathrm{N}}} \times \Big(\frac{A^{-}}{B^{-}}\mathrm{ch}\theta_{k_3+k_2-k_1} - \sqrt{\frac{s}{S}}\mathrm{sh}\theta_{k_3+k_2-k_1}\Big) - \frac{2SV_4(k_3,k_3+k_2-k_1,k_1,k_2)}{J\omega_{k_3+k_2-k_1}^{+} + \hbar\omega_{\mathrm{N}}}\Big(\frac{A^{-}}{B^{-}}\mathrm{sh}\theta_{k_3+k_2-k_1} - \sqrt{\frac{s}{S}}\mathrm{ch}\theta_{k_3+k_2-k_1}\Big). \quad (8)$$

Here, $\mathrm{ch}\theta_k \equiv \mathrm{cosh}\theta_k$, $\mathrm{sh}\theta_k \equiv \mathrm{sinh}\theta_k$, and the four-magnon exchange interaction V_i is given as

$$
\begin{aligned}
\frac{V_1(k_1,k_2,k_3,k_4)}{J} &= \Big(\cos\frac{k_4-k_2}{2}+\cos\frac{k_3-k_1}{2}\Big)\big(\mathrm{ch}\theta_{k_1}\mathrm{sh}\theta_{k_2}\mathrm{ch}\theta_{k_3}\mathrm{sh}\theta_{k_4}+\mathrm{sh}\theta_{k_1}\mathrm{ch}\theta_{k_2}\mathrm{sh}\theta_{k_3}\mathrm{ch}\theta_{k_4}\big)\\
&+\Big(\cos\frac{k_4-k_3}{2}+\cos\frac{k_2-k_1}{2}\Big)\big(\mathrm{ch}\theta_{k_1}\mathrm{ch}\theta_{k_2}\mathrm{sh}\theta_{k_3}\mathrm{sh}\theta_{k_4}+\mathrm{sh}\theta_{k_1}\mathrm{sh}\theta_{k_2}\mathrm{ch}\theta_{k_3}\mathrm{ch}\theta_{k_4}\big)\\
&-\sqrt{\frac{S}{s}}\Big[\mathrm{sh}\theta_{k_3}\mathrm{sh}\theta_{k_4}\Big(\cos\frac{k_1}{2}\mathrm{ch}\theta_{k_1}\mathrm{sh}\theta_{k_2}+\cos\frac{k_2}{2}\mathrm{sh}\theta_{k_1}\mathrm{ch}\theta_{k_2}\Big)+\mathrm{sh}\theta_{k_1}\mathrm{sh}\theta_{k_2}\Big(\cos\frac{k_3}{2}\mathrm{ch}\theta_{k_3}\mathrm{sh}\theta_{k_4}+\cos\frac{k_4}{2}\mathrm{sh}\theta_{k_3}\mathrm{ch}\theta_{k_4}\Big)\Big]\\
&-\sqrt{\frac{s}{S}}\Big[\mathrm{ch}\theta_{k_3}\mathrm{ch}\theta_{k_4}\Big(\cos\frac{k_1}{2}\mathrm{sh}\theta_{k_1}\mathrm{ch}\theta_{k_2}+\cos\frac{k_2}{2}\mathrm{ch}\theta_{k_1}\mathrm{sh}\theta_{k_2}\Big)+\mathrm{ch}\theta_{k_1}\mathrm{ch}\theta_{k_2}\Big(\cos\frac{k_3}{2}\mathrm{sh}\theta_{k_3}\mathrm{ch}\theta_{k_4}+\cos\frac{k_4}{2}\mathrm{ch}\theta_{k_3}\mathrm{sh}\theta_{k_4}\Big)\Big],\\
\frac{V_2(k_1,k_2,k_3,k_4)}{2J} &= \Big(\cos\frac{k_4-k_2}{2}+\cos\frac{k_3-k_1}{2}\Big)\big(\mathrm{ch}\theta_{k_1}\mathrm{sh}\theta_{k_2}\mathrm{ch}\theta_{k_3}\mathrm{ch}\theta_{k_4}+\mathrm{sh}\theta_{k_1}\mathrm{ch}\theta_{k_2}\mathrm{sh}\theta_{k_3}\mathrm{sh}\theta_{k_4}\big)\\
&+\Big(\cos\frac{k_4-k_3}{2}+\cos\frac{k_2-k_1}{2}\Big)\big(\mathrm{ch}\theta_{k_1}\mathrm{ch}\theta_{k_2}\mathrm{sh}\theta_{k_3}\mathrm{ch}\theta_{k_4}+\mathrm{sh}\theta_{k_1}\mathrm{sh}\theta_{k_2}\mathrm{ch}\theta_{k_3}\mathrm{sh}\theta_{k_4}\big)\\
&-\sqrt{\frac{S}{s}}\Big[\mathrm{sh}\theta_{k_3}\mathrm{ch}\theta_{k_4}\Big(\cos\frac{k_1}{2}\mathrm{ch}\theta_{k_1}\mathrm{sh}\theta_{k_2}+\cos\frac{k_2}{2}\mathrm{sh}\theta_{k_1}\mathrm{ch}\theta_{k_2}\Big)+\mathrm{sh}\theta_{k_1}\mathrm{sh}\theta_{k_2}\Big(\cos\frac{k_3}{2}\mathrm{ch}\theta_{k_3}\mathrm{ch}\theta_{k_4}+\cos\frac{k_4}{2}\mathrm{sh}\theta_{k_3}\mathrm{sh}\theta_{k_4}\Big)\Big]\\
&-\sqrt{\frac{s}{S}}\Big[\mathrm{ch}\theta_{k_3}\mathrm{sh}\theta_{k_4}\Big(\cos\frac{k_1}{2}\mathrm{sh}\theta_{k_1}\mathrm{ch}\theta_{k_2}+\cos\frac{k_2}{2}\mathrm{ch}\theta_{k_1}\mathrm{sh}\theta_{k_2}\Big)+\mathrm{ch}\theta_{k_1}\mathrm{ch}\theta_{k_2}\Big(\cos\frac{k_3}{2}\mathrm{sh}\theta_{k_3}\mathrm{sh}\theta_{k_4}+\cos\frac{k_4}{2}\mathrm{ch}\theta_{k_3}\mathrm{ch}\theta_{k_4}\Big)\Big],\\
\frac{V_3(k_1,k_2,k_3,k_4)}{4J} &= \Big(\cos\frac{k_4-k_2}{2}+\cos\frac{k_3-k_1}{2}\Big)\big(\mathrm{ch}\theta_{k_1}\mathrm{ch}\theta_{k_2}\mathrm{ch}\theta_{k_3}\mathrm{ch}\theta_{k_4}+\mathrm{sh}\theta_{k_1}\mathrm{sh}\theta_{k_2}\mathrm{sh}\theta_{k_3}\mathrm{sh}\theta_{k_4}\big)\\
&+\Big(\cos\frac{k_4-k_3}{2}+\cos\frac{k_2-k_1}{2}\Big)\big(\mathrm{ch}\theta_{k_1}\mathrm{sh}\theta_{k_2}\mathrm{sh}\theta_{k_3}\mathrm{ch}\theta_{k_4}+\mathrm{sh}\theta_{k_1}\mathrm{ch}\theta_{k_2}\mathrm{ch}\theta_{k_3}\mathrm{sh}\theta_{k_4}\big)\\
&-\sqrt{\frac{S}{s}}\Big[\mathrm{sh}\theta_{k_3}\mathrm{ch}\theta_{k_4}\Big(\cos\frac{k_1}{2}\mathrm{ch}\theta_{k_1}\mathrm{ch}\theta_{k_2}+\cos\frac{k_2}{2}\mathrm{sh}\theta_{k_1}\mathrm{sh}\theta_{k_2}\Big)+\mathrm{sh}\theta_{k_1}\mathrm{ch}\theta_{k_2}\Big(\cos\frac{k_3}{2}\mathrm{ch}\theta_{k_3}\mathrm{ch}\theta_{k_4}+\cos\frac{k_4}{2}\mathrm{sh}\theta_{k_3}\mathrm{sh}\theta_{k_4}\Big)\Big]\\
&-\sqrt{\frac{s}{S}}\Big[\mathrm{ch}\theta_{k_3}\mathrm{sh}\theta_{k_4}\Big(\cos\frac{k_1}{2}\mathrm{sh}\theta_{k_1}\mathrm{sh}\theta_{k_2}+\cos\frac{k_2}{2}\mathrm{ch}\theta_{k_1}\mathrm{ch}\theta_{k_2}\Big)+\mathrm{ch}\theta_{k_1}\mathrm{sh}\theta_{k_2}\Big(\cos\frac{k_3}{2}\mathrm{sh}\theta_{k_3}\mathrm{sh}\theta_{k_4}+\cos\frac{k_4}{2}\mathrm{ch}\theta_{k_3}\mathrm{ch}\theta_{k_4}\Big)\Big],\\
\frac{V_4(k_1,k_2,k_3,k_4)}{2J} &= \Big(\cos\frac{k_4-k_2}{2}+\cos\frac{k_3-k_1}{2}\Big)\big(\mathrm{ch}\theta_{k_1}\mathrm{sh}\theta_{k_2}\mathrm{ch}\theta_{k_3}\mathrm{ch}\theta_{k_4}+\mathrm{sh}\theta_{k_1}\mathrm{ch}\theta_{k_2}\mathrm{sh}\theta_{k_3}\mathrm{sh}\theta_{k_4}\big)\\
&+\Big(\cos\frac{k_4-k_3}{2}+\cos\frac{k_2-k_1}{2}\Big)\big(\mathrm{ch}\theta_{k_1}\mathrm{ch}\theta_{k_2}\mathrm{sh}\theta_{k_3}\mathrm{ch}\theta_{k_4}+\mathrm{sh}\theta_{k_1}\mathrm{sh}\theta_{k_2}\mathrm{ch}\theta_{k_3}\mathrm{sh}\theta_{k_4}\big)\\
&-\sqrt{\frac{S}{s}}\Big[\mathrm{ch}\theta_{k_3}\mathrm{sh}\theta_{k_4}\Big(\cos\frac{k_1}{2}\mathrm{sh}\theta_{k_1}\mathrm{ch}\theta_{k_2}+\cos\frac{k_2}{2}\mathrm{ch}\theta_{k_1}\mathrm{sh}\theta_{k_2}\Big)+\mathrm{ch}\theta_{k_1}\mathrm{ch}\theta_{k_2}\Big(\cos\frac{k_3}{2}\mathrm{sh}\theta_{k_3}\mathrm{sh}\theta_{k_4}+\cos\frac{k_4}{2}\mathrm{ch}\theta_{k_3}\mathrm{ch}\theta_{k_4}\Big)\Big]\\
&-\sqrt{\frac{s}{S}}\Big[\mathrm{sh}\theta_{k_3}\mathrm{ch}\theta_{k_4}\Big(\cos\frac{k_1}{2}\mathrm{ch}\theta_{k_1}\mathrm{sh}\theta_{k_2}+\cos\frac{k_2}{2}\mathrm{sh}\theta_{k_1}\mathrm{ch}\theta_{k_2}\Big)+\mathrm{sh}\theta_{k_1}\mathrm{sh}\theta_{k_2}\Big(\cos\frac{k_3}{2}\mathrm{ch}\theta_{k_3}\mathrm{ch}\theta_{k_4}+\cos\frac{k_4}{2}\mathrm{sh}\theta_{k_3}\mathrm{sh}\theta_{k_4}\Big)\Big].
\end{aligned}
\tag{9}
$$

We calculate the case of $(S,s)=(\frac{5}{2},\frac{1}{2})$, which is relevant to several major materials [2–4], assuming that $A^-/2 \simeq A^z \equiv A$ and $B^-/2 \simeq B^z \equiv B$. Figure 3 shows $1/T_1$ as a function of temperature and an applied magnetic field. All in all, the exchange-scattering-enhanced three-magnon relaxation rate $1/T_1^{(3)}$ grows with increasing temperature and decreasing field and ends in the leading contribution to $1/T_1$. The temperature dependence of $1/T_1$ is determined by $\bar{n}_k^-$ unless temperature is sufficiently high. As temperature increases, $\bar{n}_k^-$ is decreasing at $k \simeq 0$ but otherwise increasing [23]. $|\mathrm{d}\omega_k^-/\mathrm{d}k|_{k=k_2^-}^{-1}$ makes the $k_1 \simeq 0$ components predominant in the momentum summation (5), while such predominance arising from $|\mathrm{d}\omega_k^-/\mathrm{d}k|_{k=k_3^-}^{-1}$ is suppressed in the double summation (6). $1/T_1^{(2)}$ and $1/T_1^{(3)}$ are hence decreasing and increasing, respectively, with increasing temperature and therefore, the Raman-to-three-magnon crossover may be detected at low fields.

The field dependence of $1/T_1$ is also useful in detecting the crossover. At moderately low temperatures and weak fields, $\hbar\omega_\mathrm{N} \ll k_\mathrm{B}T \ll J$, we may evaluate Eq. (5) as

$$
\frac{1}{T_1^{(2)}} \simeq \frac{2(g\mu_\mathrm{B}\hbar\gamma_\mathrm{N})^2(AS-Bs)^2}{\pi\hbar Ss(S-s)J}\mathrm{e}^{-g\mu_\mathrm{B}H/k_\mathrm{B}T}K_0\Big(\frac{\hbar\omega_\mathrm{N}}{2k_\mathrm{B}T}\Big),
\tag{10}
$$

where K_0 is the modified Bessel function of the second kind and behaves as $K_0(\hbar\omega_\mathrm{N}/2k_\mathrm{B}T) \simeq 0.80908 - \ln(\hbar\omega_\mathrm{N}/k_\mathrm{B}T)$ for $\hbar\omega_\mathrm{N} \ll k_\mathrm{B}T$. Considering the relation $\omega_\mathrm{N} = \gamma_\mathrm{N}H$, we find that the field dependence of $1/T_1^{(2)}$ is logarithmic at weak fields and turns exponential with increasing field. Since $1/T_1^{(3)}$ exhibits much stronger initial field dependence, the three-magnon relaxation can be detected at weak fields. We plot *the crossover points* in Fig. 4. The three-magnon relaxation process generally predominates over the Raman one at high temperatures and weak fields. Since the ferrimagnetic nuclear spin-

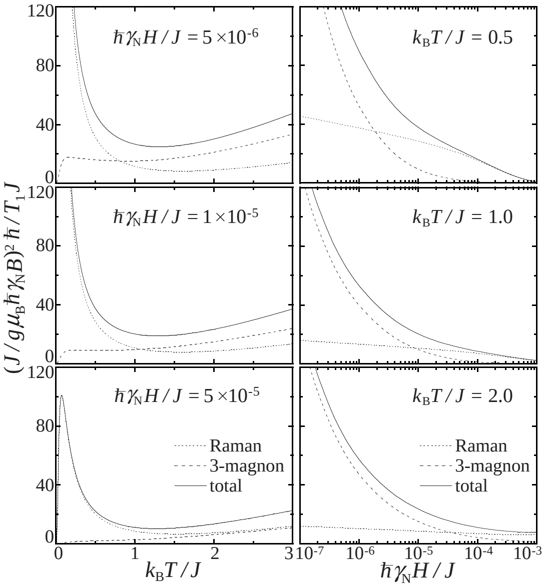

FIG. 3. Modified spin-wave calculations of the temperature (the left three) and field (the right three) dependences of the nuclear spin-lattice relaxation rate at $A/B = 0.1$, where $1/T_1^{(2)}$ and $1/T_1^{(3)}$ are plotted by dotted and broken lines, respectively, while $1/T_1^{(2)} + 1/T_1^{(3)} \equiv 1/T_1$, which is observable, by solid lines.

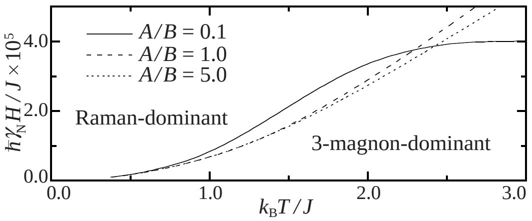

FIG. 4. The crossover point, where $1/T_1^{(2)} = 1/T_1^{(3)}$, as a function of temperature and an applied field.

lattice relaxation is very sensitive to another adjustable parameter A/B, that is, the location of the probe nuclei, any T_1 measurement should be accompanied by detailed structural analyses. At the special location of $A/B \sim (d_s/d_S)^3 \simeq s/S$, where d_S (d_s) is the distance between the nuclear and larger (smaller) electronic spins, the leading ferromagnetic spin waves are almost invisible to the nuclear spins [16,23] and therefore $1/T_1$ is too small to be measured. The three-magnon-dominant relaxation rate is detectable for $A/B = 0.1$ and $A/B = 5.0$, for exmaple, which are relevant to ^{1}H nuclei in MnCu(pbaOH)(H_2O)$_3$ with $J/k_B \simeq 34\,\mathrm{K}$ [3] and ^{19}F nuclei in Mn(hfac)$_2$NITiPr with $J/k_B \simeq 460\,\mathrm{K}$ [4], respectively. When we measure MnCu(pbaOH)(H_2O)$_3$ and Mn(hfac)$_2$NITiPr at 100 K and room temperature, respectively, the three-magnon relaxation is possibly dominant for $H \lesssim 0.6\,\mathrm{T}$ in both compounds.

There exist pioneering T_1 measurements on the layered ferromagnet $CrCl_3$ [24] and the coupled-chain antiferromagnet $CsMnCl_3\cdot 2H_2O$ [25], which give evidence of the relevant three-magnon relaxation process in accordance with the Pincus-Beeman formulation [18]. However, they are both low-temperature measurements under the existing three-dimensional long-range order. A similarly-motivated experiment on the one-dimensional easy-plane ferromagnet $CsNiF_3$ [26] was performed at higher temperatures but explained in terms of solitons, possibly because of the lack of the spin-wave formulation in one dimension. Here is a modern theoretical tool—the modified spin-wave theory based on the new scheme [12]. Let us observe the three-magnon nuclear-spin scattering in the one-dimensional quantum relaxation.

The authors are grateful to Professor T. Goto for valuable comments. This work was supported by the Ministry of Education, Culture, Sports, Science and Technology of Japan and the Nissan Science Foundation.

---

[1] O. Kahn, Y. Pei, and Y. Journaux, in *Inorganic Materials*, edited by D. W. Bruce and D. O'Hare (Wiley, New York, 1995), p. 95.

[2] A. Gleizes and M. Verdaguer, J. Am. Chem. Soc. **103**, 7373 (1981); **106**, 3727 (1984).

[3] Y. Pei, M. Verdaguer, O. Kahn, J. Sletten, and J.-P. Renard, Inorg. Chem. **26**, 138 (1987); O. Kahn, Y. Pei, M. Verdaguer, J. P. Renard, and J. Sletten, J. Am. Chem. Soc. **110**, 782 (1988).

[4] A. Caneschi, D. Gatteschi, P. Rey, and R. Sessoli, Inorg. Chem. **27**, 1756 (1988); A. Caneschi, D. Gatteschi, J.-P. Renard, P. Rey, and R. Sessoli, *ibid.* **28**, 1976 (1989).

[5] D. Shiomi, K. Sato, and T. Takui, J. Phys. Chem. B **104**, 1961 (2000).

[6] Y. Hosokoshi, K. Katoh, Y. Nakazawa, H. Nakano, and K. Inoue, J. Am. Chem. Soc. **123**, 7921 (2001).

[7] A. Escuer, R. Vicente, M. S. El Fallah, M. A. S. Goher, and F. A. Mautner, Inorg. Chem. **37**, 4466 (1998).

[8] M. Drillon, M. Belaiche, P. Legoll, J. Aride, A. Boukhari, and A. Moqine, J. Magn. Magn. Mater. **128**, 83 (1993).

[9] M. Verdaguer, A. Gleizes, J. P. Renard, and J. Seiden, Phys. Rev. B **29**, 5144 (1984).

[10] M. Drillon, E. Coronado, R. Georges, J. C. Gianduzzo, and J. Curely, Phys. Rev. B **40**, 10992 (1989).

[11] S. K. Pati, S. Ramasesha, and D. Sen, Phys. Rev. B **55**, 8894 (1997); J. Phys.: Condens. Matter **9**, 8707 (1997).

[12] S. Yamamoto and T. Fukui, Phys. Rev. B **57**, R14008 (1998); S. Yamamoto, T. Fukui, K. Maisinger, and U. Schollwöck, J. Phys.: Condens. Matter **10**, 11033 (1998).

[13] S. Yamamoto, Phys. Rev. B **59**, 1024 (1999).

[14] A. S. Ovchinnikov, I. G. Bostrem, V. E. Sinitsyn, A. S. Boyarchenkov, N. V. Baranov, and K. Inoue, J. Phys.: Condens. Matter **14**, 8067 (2002).

[15] S. Yamamoto and T. Sakai, J. Phys. Soc. Jpn. **67**, 3711 (1998).

[16] H. Hori and S. Yamamoto, Phys. Rev. B **68**, 054409 (2003).

[17] V. S. Viswanath and G. Müller, *The Recursion Method*

(Springer-Verlag, Berlin, 1994), p. 136.

[18] P. Pincus, Phys. Rev. Lett. **16**, 398 (1966); D. Beeman and P. Pincus, Phys. Rev. **166**, 359 (1968).

[19] S. Yamamoto and T. Nakanishi, Phys. Rev. Lett. **89**, 157603 (2002).

[20] M. Takahashi, Phys. Rev. B **40**, 2494 (1989).

[21] J. E. Hirsch and S. Tang, Phys. Rev. B **40**, 4769 (1989); S. Tang, M. E. Lazzouni, and J. E. Hirsch, Phys. Rev. B **40**, 5000 (1989).

[22] S. Yamamoto, Phys. Rev. B **69**, 064426 (2004).

[23] S. Yamamoto, J. Phys. Soc. Jpn. **69**, 2324 (2000).

[24] A. Narath and A. T. Fromhold, Jr., Phys. Rev. Lett. **17**, 354 (1966).

[25] H. Nishihara, W. J. M. de Jonge, and T. de Neef, Phys. Rev. B **12**, 5325 (1975).

[26] T. Goto, Phys. Rev. B **28**, 6347 (1983).